Progress In Electromagnetics Research, **PIER 16, 67–85, 1997**

GAUSSIAN BEAM SCATTERING FROM A SEMICIRCULAR CHANNEL IN A CONDUCTING PLANE

T. Shen, W. Dou, and Z. Sun

State Key Laboratory of Millimeter Waves
Southeast University
Nanjing, Jiangsu 210096
P. R. China

1. INTRODUCTION

Electromagnetic scattering from a cracked conducting plane is an important topic in the study of rough surface scattering, nondestructive testing for metal fatigue, electromagnetic diffraction computation, etc. The problem of plane wave scattering from a semicircular channel or the one loaded by a single or multilayer concentric dielectric circular cylinder as well as a dielectric coated conducting cylinder in a conducting plane has been studied extensively by Sachdeva and Hurd [1], Hinders and Yaghjian [2], Park et al. [3,4], and Ragheb [5]. However, for some practical electromagnetic scattering problems, the effect of the incident wave shape sometimes becomes significant, depending on the antenna type, the target size, and the distance between the antenna and the target. Therefore, a more realistic assumption of the wave shape, such as a Gaussian beam or a spherical wave, is required for the accurate prediction of scattering behaviors.

With the problem of Gaussian beam scattering from a conducting cylinder investigated, Kozaki [6] has derived a Gaussian beam approximate expression in the simple form of a single series. Each term in the series is a product of a well-known cylindrical harmonic wave function and a weighting coefficient. Recently, the problem of Gaussian beam scattering from a semicircular boss above a conducting plane, a structure analogous to the one studied in this paper, has been investigated by Eom et al. [7] with the Kozaki's Gaussian beam approximate expression and the method of image superposition.

In this paper, a dual series solution to the problem of Gaussian beam scattering from a semicircular channel in a conducting plane is presented. The usual procedure used here is similar to that given in [2]. However, since the incident wave is a Gaussian beam instead of a plane wave, the Kozaki's Gaussian beam approximate expression is introduced. The present treatment is more general, while the plane wave scattering is only its special case.

2. FORMULATION

Figure 1 shows the geometry of the two-dimensional problem. For the sake of convenience, three coordinate systems, i.e., two rectangular coordinate systems, (x, y, z) and (x_1, y_1, z), and one cylindrical coordinate system, (r, ϕ, z), are defined. The origins of the three coordinate systems are all located at the center of the semicircular channel, and the coordinate system (x_1, y_1, z) rotates an angle ϕ_0 clockwise with respect to the coordinate system (x, y, z). The radius of the semicircular channel embedded along the z-axis in the conducting plane is a. A Gaussian beam whose source is located at $(x_1 = -r_0,\ y_1 = 0)$ is incident on it, making an angle ϕ_0 (incident angle) clockwise with respect to the negative x-axis. The whole space above the conducting plane is divided into two regions: region I $(r \geq a,\ 0 < \phi < \pi)$ and region II $(r \leq a)$. Throughout this paper, the time dependence $\exp(j\omega t)$ is assumed and suppressed.

A. TM case

For the TM case, the z-component of the electric field of the incident Gaussian beam source is assumed as

$$E_z^{inc}(x_1 = -r_0, y_1) = E_0 \exp\left(-\beta^2 y_1^2\right), \tag{1}$$

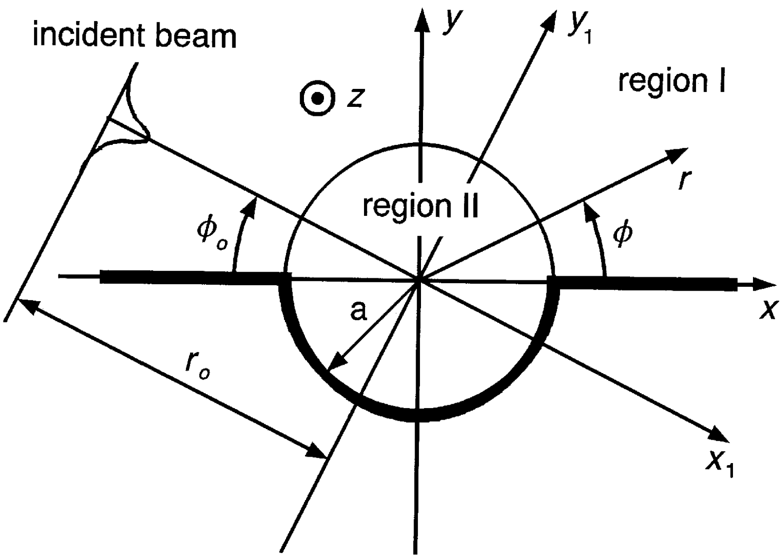

Figure 1. Geometry of the problem.

where

$$\beta^2 = a_0^2 + jb_0^2, \tag{2}$$

$1/|\beta|$ corresponds to the beamwidth, and E_0 is the arbitrary electric field amplitude. The incident electric field from the beam source can be approximately expanded as [6]

$$E_z^{inc}(r,\phi) = E_0 \sum_{n=0}^{\infty} A_n \varepsilon_n j^{-n} J_n(kr) \cos n(\phi + \phi_0), \tag{3}$$

where

$$A_n \approx \frac{\exp(-jkr_0)}{\sqrt{1-jZ_0}} \exp\left[-\left(\frac{n\beta}{k}\right)^2 \frac{1}{1-jZ_0}\right]\left[1 - 2\left(\frac{\beta}{k\sqrt{1-jZ_0}}\right)^4 n^2 + \frac{4}{3}\left(\frac{\beta}{k\sqrt{1-jZ_0}}\right)^6 n^4 + \cdots\right], \tag{4}$$

$$Z_0 = \frac{2\beta^2 r_0}{k}, \tag{5}$$

$\varepsilon_n = 1$ for $n = 0$ and 2 for $n \geq 1$, $k = 2\pi/\lambda$ is the free space wavenumber and λ is the free space wavelength, and J_n is the Bessel function of the first kind and order n. Note that (3) is the approximate expansion of the incident Gaussian beam, which is valid for $|(\beta\lambda)^2| < 0.3$ [6].

The scattered electric field in region I can be decomposed into two parts: the reflected and the diffracted fields, which are expanded as

$$E_z^{ref}(r,\phi) = -E_0 \sum_{n=0}^{\infty} A_n \varepsilon_n j^{-n} J_n(kr) \cos n(\phi - \phi_0), \tag{6}$$

$$E_z^{dif}(r,\phi) = E_0 \sum_{n=1}^{\infty} B_n^{TM} H_n^{(2)}(kr) \sin n\phi, \tag{7}$$

where B_n^{TM} are the unknown mode coefficients, and $H_n^{(2)}$ is the Hankel function of the second kind and order n.

In region II, the electric field is expanded as

$$E_z^{int}(r,\phi) = E_0 \sum_{n=0}^{\infty} J_n(kr) \Big(C_n^{TM} \cos n\phi + D_n^{TM} \sin n\phi \Big) \quad \Big(D_0^{TM} = 0 \Big), \tag{8}$$

where C_n^{TM} and D_n^{TM} are the unknown mode coefficients.

From

$$H_\phi(r,\phi) = \frac{1}{j\omega\mu} \frac{\partial E_z(r,\phi)}{\partial r}, \tag{9}$$

the ϕ-component of the magnetic field can be derived.

In order to calculate the unknown mode coefficients, the boundary conditions of the zero tangential electric field (i.e., E_z) at $r = a$ and $\pi < \phi < 2\pi$, and continuous tangential electric and magnetic fields (i.e., E_z and H_ϕ) across the imaginary aperture $r = a$ and $0 < \phi < \pi$, are enforced, which yields

$$\sum_{n=1}^{\infty} D_n^{TM} J_n(ka) \sin n\phi = -\sum_{n=0}^{\infty} C_n^{TM} J_n(ka) \cos n\phi \quad (\pi < \phi < 2\pi), \tag{10}$$

$$\sum_{n=1}^{\infty}\left[-4A_n j^{-n} J_n(ka)\sin n\phi_0 + B_n^{TM} H_n^{(2)}(ka) - D_n^{TM} J_n(ka)\right]\sin n\phi$$
$$=\sum_{n=0}^{\infty} C_n^{TM} J_n(ka)\cos n\phi \quad (0<\phi<\pi), \tag{11}$$

$$\sum_{n=1}^{\infty}\left[-4A_n j^{-n} J_n'(ka)\sin n\phi_0 + B_n^{TM} H_n^{(2)\prime}(ka) - D_n^{TM} J_n'(ka)\right]\sin n\phi$$
$$=\sum_{n=0}^{\infty} C_n^{TM} J_n'(ka)\cos n\phi \quad (0<\phi<\pi), \tag{12}$$

where the prime denotes the derivative with respect to the argument. Substituting $\pi+\phi$ $(0<\phi<\pi)$ for ϕ in (10), (10)–(12) can be written in the unified form

$$\sum_{n=1}^{\infty} f_n \sin n\phi = \sum_{n=0}^{\infty} g_n \cos n\phi \quad (0<\phi<\pi). \tag{13}$$

Multiplying (13) by $\sin m\phi$ $(m\geq 1)$ and integrating both sides with respect to ϕ from 0 to π yields

$$f_m = \frac{4m}{\pi} \sum_{\substack{n=0\\ n+m=\mathrm{odd}}}^{\infty} \frac{1}{m^2-n^2} g_n \quad (m\geq 1), \tag{14}$$

where $\sum\limits_{\substack{n=0\\ n+m=\mathrm{odd}}}^{\infty}$ represents the summation with respect to n from 0 to infinite which satisfies $n+m=$odd. Employing (14) in (10)-(12) with the necessary mathematical manipulation yields

$$\sum_{\substack{n=0\\ n+m=\mathrm{odd}}}^{\infty} \frac{1}{m^2-n^2}\left\{J_n(ka) + \frac{j\pi ka}{2}\left[J_m(ka)H_m^{(2)\prime}(ka)J_n(ka)\right.\right.$$
$$\left.\left. - J_m(ka)H_m^{(2)}(ka)J_n'(ka)\right]\right\}C_n^{TM}$$
$$=\frac{-\pi A_m j^{-m} J_m(ka)\sin m\phi_0}{m} \qquad (m\geq 1), \tag{15}$$

$$B_m^{TM} = \frac{4}{H_m^{(2)}(ka)} \left[\frac{2m}{\pi} \sum_{\substack{n=0 \\ n+m=\text{odd}}}^{\infty} \frac{J_n(ka)}{m^2 - n^2} C_n^{TM} \right.$$
$$\left. + A_m j^{-m} J_m(ka) \sin m\phi_0 \right] \qquad (m \geq 1). \quad (16)$$

Equation 15 can be solved numerically to obtain the C_n^{TM}. In practical computation, the infinite series involved in the solution must be truncated after a certain number of terms, under the prerequisite of achieving the solution convergence. Once the C_n^{TM} are obtained, the B_n^{TM} can then be calculated from (16).

B. TE case

For the TE case, in a similar fashion, the z-components of the incident, the reflected, and the diffracted magnetic fields in region I are expanded as

$$H_z^{inc}(r,\phi) = H_0 \sum_{n=0}^{\infty} A_n \varepsilon_n j^{-n} J_n(kr) \cos n(\phi + \phi_0), \qquad (17)$$

$$H_z^{ref}(r,\phi) = H_0 \sum_{n=0}^{\infty} A_n \varepsilon_n j^{-n} J_n(kr) \cos n(\phi - \phi_0), \qquad (18)$$

$$H_z^{dif}(r,\phi) = H_0 \sum_{n=0}^{\infty} B_n^{TE} H_n^{(2)}(kr) \cos n\phi, \qquad (19)$$

where H_0 is the arbitrary magnetic field amplitude, and B_n^{TE} are the unknown mode coefficients.

In region II, the magnetic field is expanded as

$$H_z^{int}(r,\phi) = H_0 \sum_{n=0}^{\infty} J_n(kr) \Big(C_n^{TE} \cos n\phi + D_n^{TE} \sin n\phi \Big) \quad \Big(D_0^{TE} = 0 \Big), \qquad (20)$$

where C_n^{TE} and D_n^{TE} are the unknown mode coefficients.

From

$$E_\phi(r,\phi) = \frac{j}{\omega\varepsilon}\frac{\partial H_z(r,\phi)}{\partial r}, \tag{21}$$

the ϕ-component of the electric field can be derived.

In order to calculate the unknown mode coefficients, the boundary conditions of the zero tangential electric field (i.e., E_ϕ) at $r = a$ and $\pi < \phi < 2\pi$, and continuous tangential electric and magnetic fields (i.e., E_ϕ and H_z) across the imaginary aperture $r = a$ and $0 < \phi < \pi$, are enforced. Then following the same procedure as in the TM case, it can be found eventually that

$$\sum_{\substack{n=1\\ n+m=\mathrm{odd}}}^{\infty} \frac{n}{n^2-m^2}\left\{J_n'(ka) + \frac{j\pi ka}{2}\left[J_m'(ka)H_m^{(2)'}(ka)J_n(ka) - J_m'(ka)H_m^{(2)}(ka)J_n'(ka)\right]\right\}D_n^{TE} = \pi A_m j^{-m} J_m'(ka)\cos m\phi_0 \quad (m \geq 0), \tag{22}$$

$$B_m^{TE} = \frac{2\varepsilon_m}{H_m^{(2)'}(ka)}\left[\frac{2}{\pi}\sum_{\substack{n=1\\ n+m=\mathrm{odd}}}^{\infty} \frac{nJ_n'(ka)}{n^2-m^2}D_n^{TE} - A_m j^{-m} J_m'(ka)\cos m\phi_0\right] \qquad (m \geq 0). \tag{23}$$

Equation 22 can be solved numerically to obtain the D_n^{TE}. Once the D_n^{TE} are obtained, the B_n^{TE} can then be calculated from (23).

The scattering properties of a two-dimensional cylindrical object of infinite length are conveniently described in terms of the scattering width W, which is defined as

$$W(\phi) = \lim_{r\to\infty} 2\pi r\left|\frac{\begin{smallmatrix}E_z^{dif}\\ H_z^{dif}\end{smallmatrix}(r,\phi)}{\begin{smallmatrix}E_z^{inc}\\ H_z^{inc}\end{smallmatrix}(a,\pi-\phi_0)}\right|^2. \tag{24}$$

Use of the large argument approximation of the Hankel function reduces (24) to

$$W(\phi) = \frac{2\lambda}{\pi} \left| \frac{P(\phi)}{\sum\limits_{n=0}^{\infty} A_n \varepsilon_n j^n J_n(ka)} \right|^2, \tag{25}$$

where

$$P(\phi) = \sum_{n=0}^{\infty} j^n \begin{matrix} B_n^{TM} \sin n\phi \\ B_n^{TE} \cos n\phi \end{matrix} \tag{26}$$

is the scattered field pattern. The backscattering width W_b can be obtained from (25) at $\phi = \pi - \phi_0$.

3. NUMERICAL RESULTS

In order to verify the above formulation, the plane wave incidence case is first considered. For the plane wave incidence case, both a_0 and b_0 are set to be zero, while r_0/λ can be taken as an arbitrary value greater than 0, which has no influence on the result. Figure 2 shows the backscattering width W_b versus incident angle ϕ_0 with $ka = 4\pi$. An excellent agreement is achieved between the results in this paper and their correspondences in [5].

As mentioned above, the infinite series involved in the solution must be truncated after a certain number of terms, under the prerequisite of achieving the solution convergence. Table I lists the backscattering width W_b versus the integer N which is the number of series terms used in the computation for eight different combinations of TM, TE, plane wave (denoted by P), Gaussian beam (denoted by G) incidence cases, and two different values of ka, with $\phi_0 = 90^\circ$, and $r_0/\lambda = 10$, $(a_0\lambda)^2 = 0.053$, and $(b_0\lambda)^2 = 0.236$ for the Gaussian beam. Note that the results for even N are not listed here since they are the same as those for odd $(N-1)$. The Gaussian beam beamwidth parameters used here correspond to those of the X-band transmitter presented in [6]. For $ka = 5$, only 17 series terms are needed to achieve the solution convergence for four different incidence cases, whereas for $ka = 15$, 33 series terms are needed. In general, the number of the series terms used in the computation depends on the value of ka (i.e., channel radius): the larger ka is, the more series terms are needed in the computation to achieve the solution convergence.

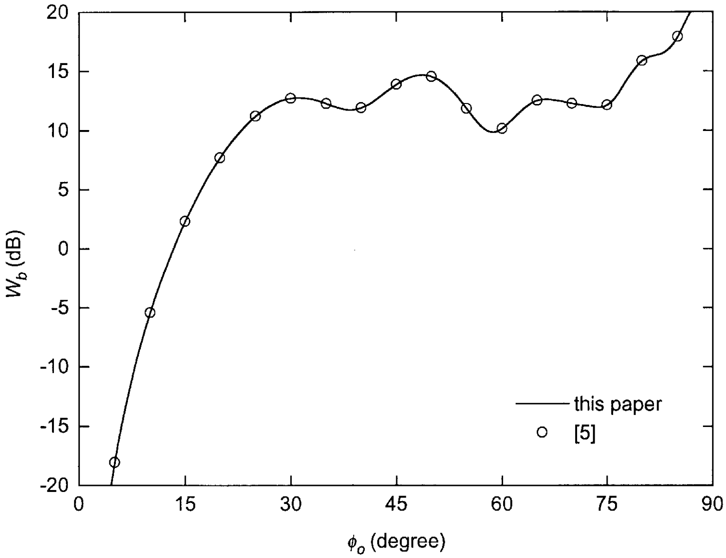

(a)

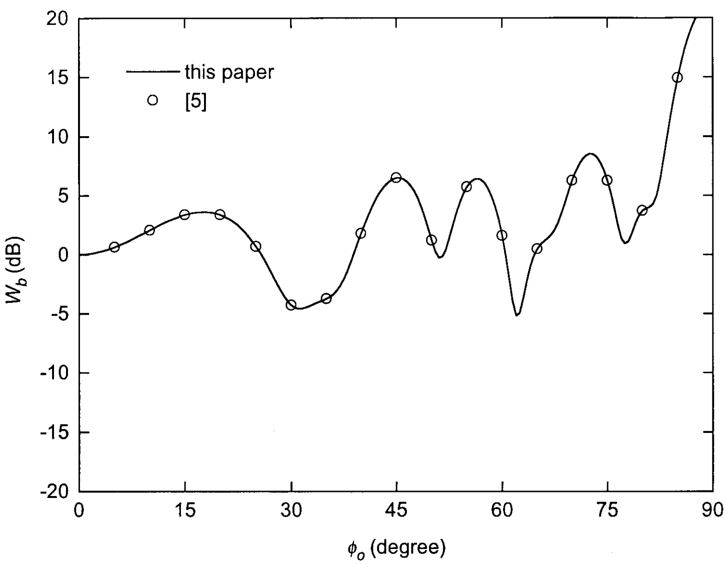

(b)

Figure 2. Backscattering width W_b versus incident angle ϕ_0 (plane wave incidence case) with $ka = 4\pi$. (a) TM case. (b) TE case.

	W_b (dB)							
	ka=5				ka=15			
	TM		TE		TM		TE	
N	G	P	G	P	G	P	G	P
1	8.45674	8.61321	3.67592	3.82882	9.59519	10.07441	3.46123	3.93690
3	15.35776	15.52568	11.68622	11.86765	15.51514	16.00806	12.70617	13.19976
5	18.43884	18.63079	12.23934	12.47891	17.72199	18.30978	16.36231	16.90699
7	18.61731	18.80246	12.24597	12.51943	17.73034	18.30117	16.89175	17.51717
9	18.40257	18.58186	12.20123	12.48726	18.05252	18.11133	19.29628	19.84704
11	18.29471	18.47107	12.17143	12.46278	21.76580	22.66050	21.37480	21.78841
13	18.23762	18.41239	12.15196	12.44622	22.86442	24.14538	23.06030	23.54977
15	18.20169	18.37546	12.13838	12.43451	23.10384	24.66250	23.81400	24.46662
17	18.17670	18.34980	12.12842	12.42584	23.05459	24.65732	24.10053	24.85245
19					22.94961	24.52092	24.20160	24.99928
21					22.88639	24.42726	24.24531	25.06394
23					22.85331	24.37597	24.27055	25.10043
25					22.83408	24.34642	24.28779	25.12481
27					22.82171	24.32766	24.30050	25.14256
29					22.81323	24.31482	24.31029	25.15611
31					22.80716	24.30557	24.31805	25.16680
33					22.80268	24.29866	24.32434	25.17546

Table I. Backscattering width W_b versus N with $\phi_0 = 90°$, and $r_0/\lambda = 10$, $(a_0\lambda)^2 = 0.053$, and $(b_0\lambda)^2 = 0.236$ for the Gaussian beam. P and G denote plane wave and Gaussian beam incidence cases respectively.

In order to further verify the formulation in Section II and the choice criterion of the number of series terms used in the computation discussed above, another example is considered. Figure 3 shows the scattered field amplitude $|P(\phi)|$ versus ka at three different scattering angles for the plane wave normal incidence case. Once again, an excellent agreement is achieved between the results in this paper and their correspondences in [3] for TM case and [4] for TE case. Note that the number of series terms used in the computation varies with the value of ka.

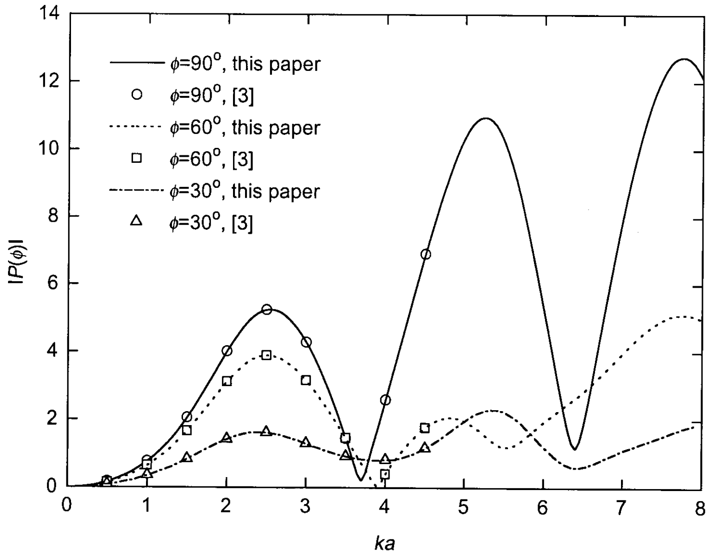

(a)

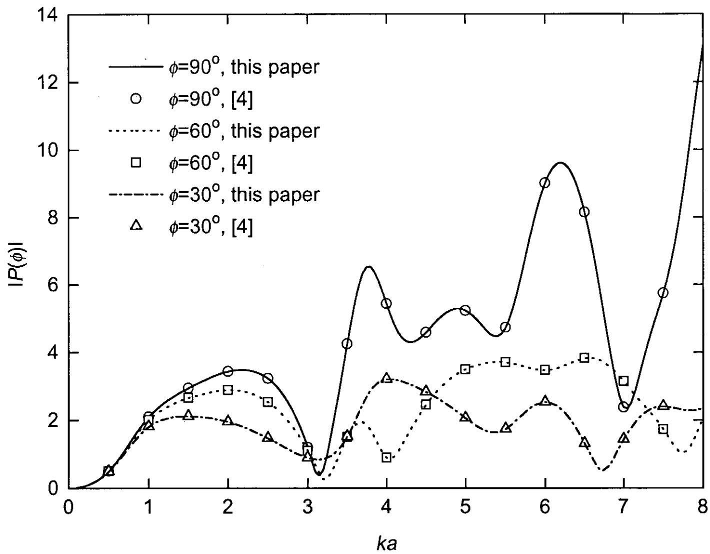

(b)

Figure 3. Scattered field amplitude $|P(\phi)|$ versus ka at three different scattering angles (plane wave incidence case) with $\phi_0 = 90°$. (a) TM case. (b) TE case.

Figures 4 and 5 show the scattering width W versus scattering angle ϕ for $\phi_0 = 90°$ and $\phi_0 = 60°$ respectively, for both Gaussian beam and plane wave incidence cases, with $ka = 9\pi$, and $r_0/\lambda = 10$, $(a_0\lambda)^2 = 0.053$, and $(b_0\lambda)^2 = 0.236$ for the Gaussian beam. There is a significant difference between Gaussian beam and plane wave scattering behaviors. This is because the Gaussian beam incident on the semicircular channel is no longer as uniformly distributed as the infinitely extended uniform plane wave. In addition, the Gaussian beam *backward* scattering width is lower than the plane wave one.

Figures 6 and 7 show the backscattering width W_b versus incident angle ϕ_0 for $ka = 9\pi$ and $ka = \pi$ respectively, for both Gaussian beam and plane wave incidence cases, with $r_0/\lambda = 10$, $(a_0\lambda)^2 = 0.053$, and $(b_0\lambda)^2 = 0.236$ for the Gaussian beam. For $ka = 9\pi$, generally speaking, the Gaussian beam scattering behavior is totally different from the plane wave one although they are about the same for the TM case when the incident angle ϕ_0 is less than $15°$. However, for $ka = \pi$, the Gaussian beam scattering behavior is nearly all the same as the plane wave one. This is because for the semicircular channel of smaller size, the incident Gaussian beam is nearly uniformly distributed as the plane wave. This point can be further supported by the following two examples.

Figures 8 and 9 show the scattering width W versus ka at two different scattering angles for $\phi_0 = 90°$ and $\phi_0 = 30°$ respectively, for both Gaussian beam and plane wave incidence cases, with $r_0/\lambda = 10$, $(a_0\lambda)^2 = 0.053$, and $(b_0\lambda)^2 = 0.236$ for the Gaussian beam. When ka (i.e., semicircular channel radius) is small, Gaussian beam and plane wave scattering behaviors are nearly all the same, whereas the difference between them becomes large gradually with ka increasing.

4. CONCLUSION

A dual series solution to the problem of Gaussian beam scattering from a semicircular channel in a conducting plane was presented. The problem was solved by the boundary value method together with the Kozaki's Gaussian beam approximate expression. Some numerical results were shown. Differences between Gaussian beam and plane wave scattering behaviors were discussed. The present treatment could be easily extended to the problem of Gaussian beam scattering from the same structure loaded by a single or multilayer dielectric circular cylinder.

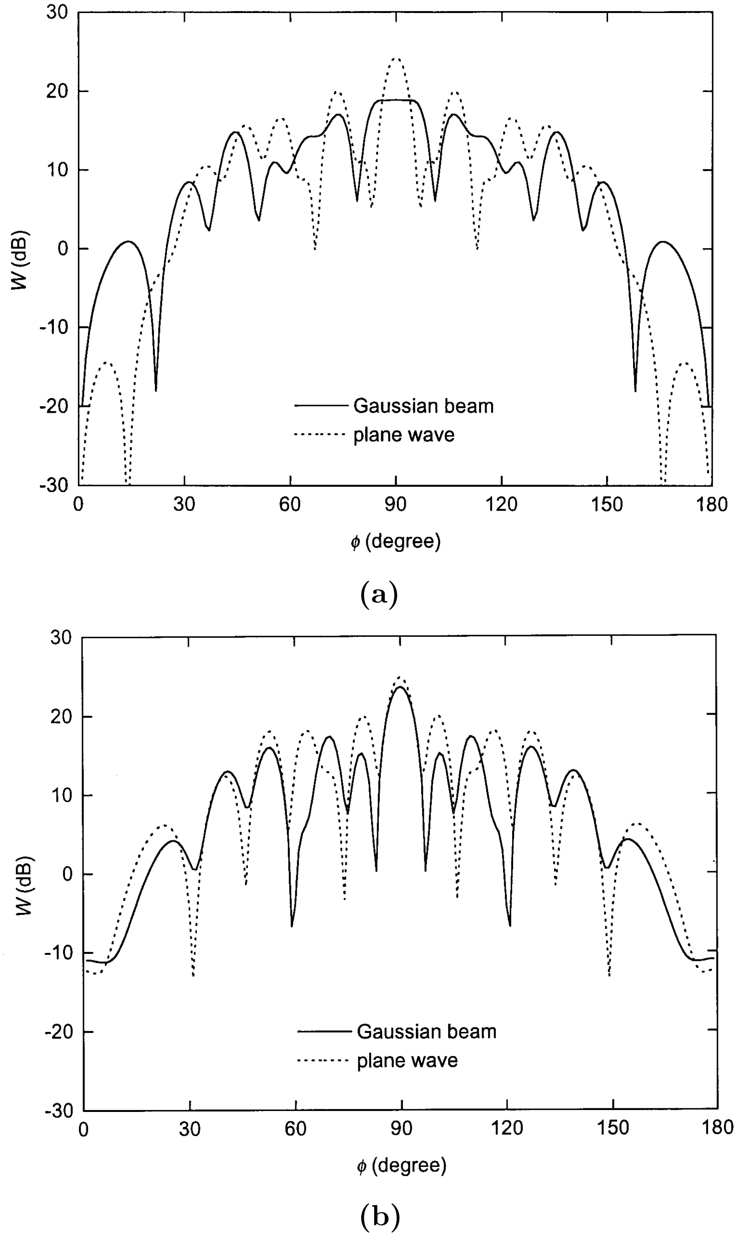

Figure 4. Scattering width W versus scattering angle ϕ with $\phi_0 = 90^\circ$, $ka = 9\pi$, and $r_0/\lambda = 10$, $(a_0\lambda)^2 = 0.053$, and $(b_0\lambda)^2 = 0.236$ for the Gaussian beam. (a) TM case. (b) TE case.

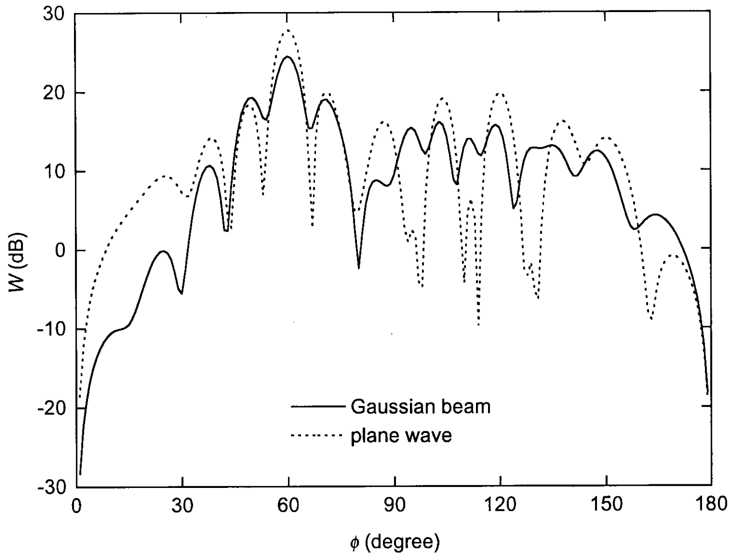

(a)

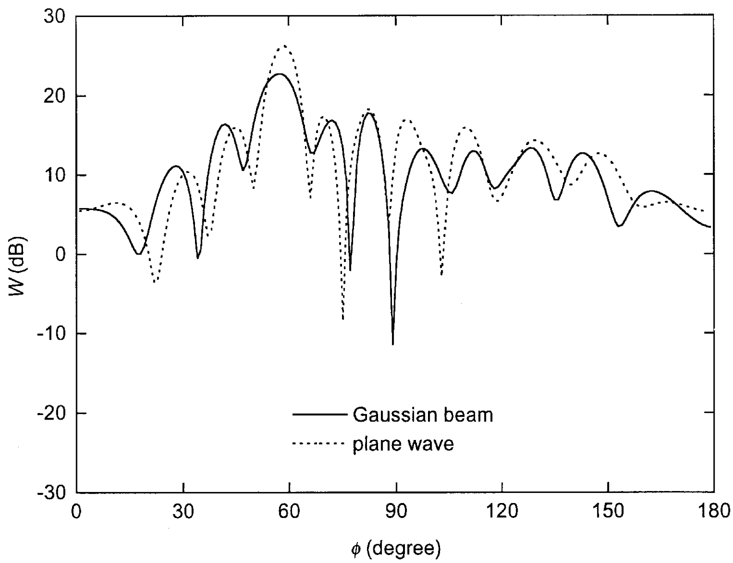

(b)

Figure 5. Scattering width W versus scattering angle ϕ with $\phi_0 = 60^\circ$, $ka = 9\pi$, and $r_0/\lambda = 10$, $(a_0\lambda)^2 = 0.053$, and $(b_0\lambda)^2 = 0.236$ for the Gaussian beam. (a) TM case. (b) TE case.

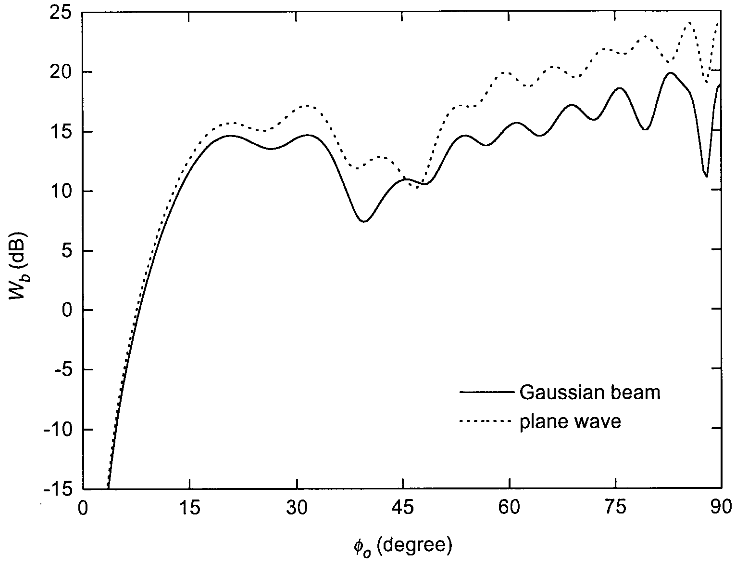

(a)

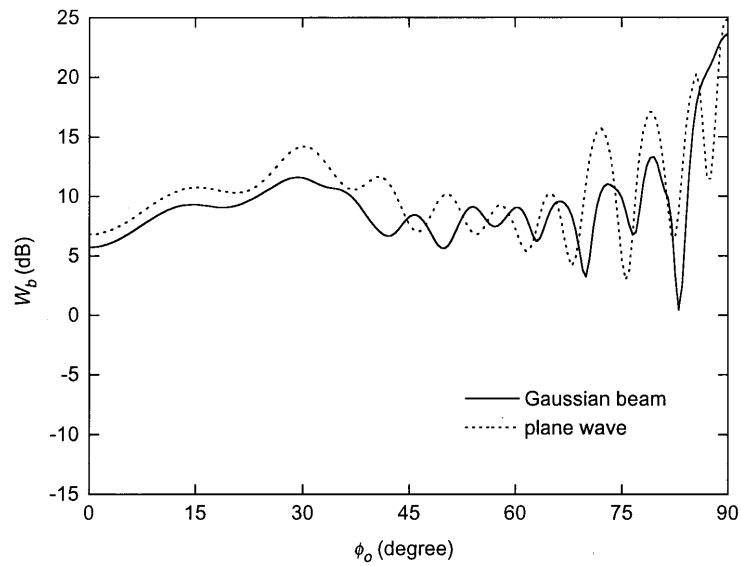

(b)

Figure 6. Backscattering width W_b versus incident angle ϕ_0 with $ka = 9\pi$, and $r_0/\lambda = 10$, $(a_0\lambda)^2 = 0.053$, and $(b_0\lambda)^2 = 0.236$ for the Gaussian beam. (a) TM case. (b) TE case.

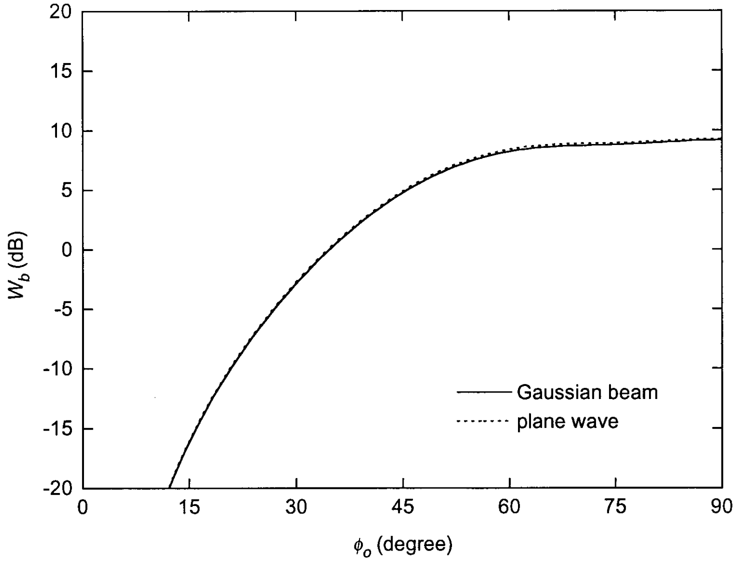

(a)

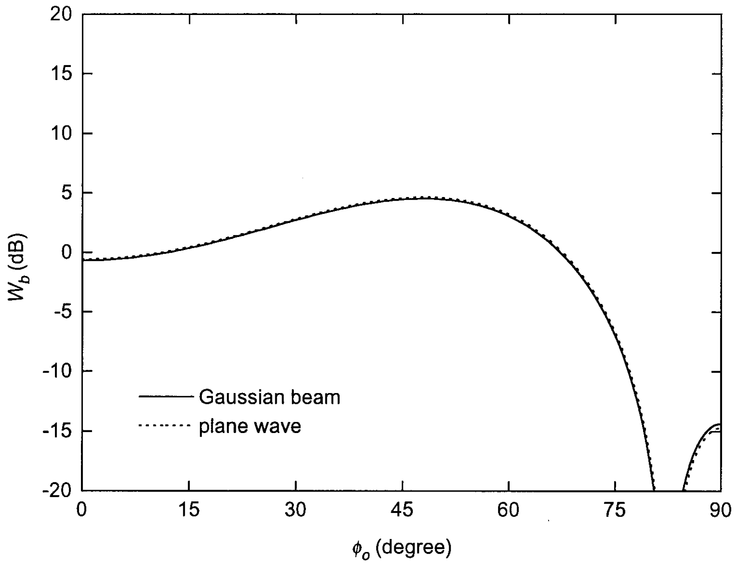

(b)

Figure 7. Backscattering width W_b versus incident angle ϕ_0 with $ka = \pi$, and $r_0/\lambda = 10$, $(a_0\lambda)^2 = 0.053$, and $(b_0\lambda)^2 = 0.236$ for the Gaussian beam. (a) TM case. (b) TE case.

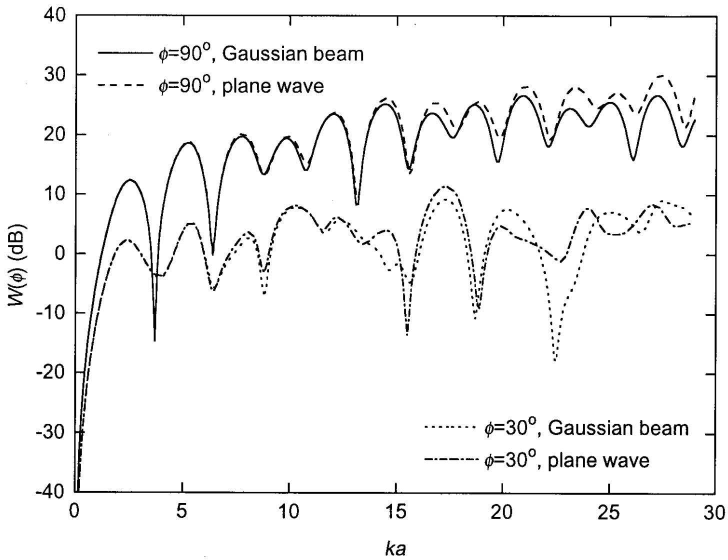

(a)

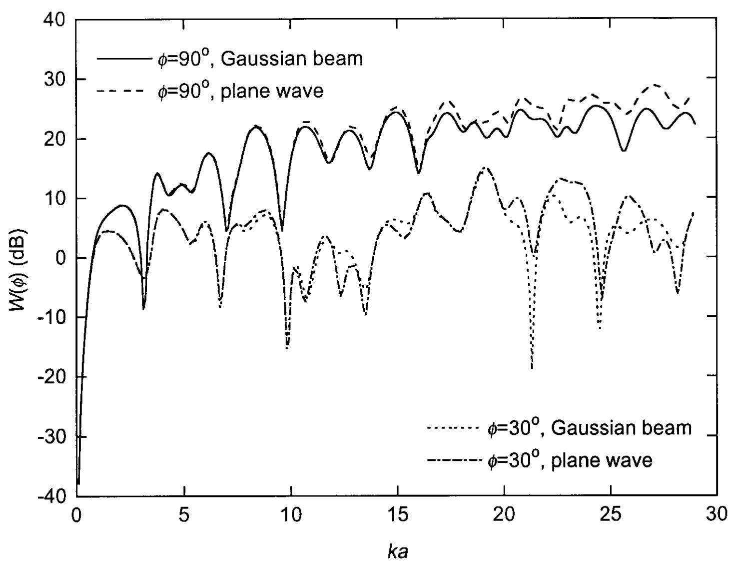

(b)

Figure 8. Scattering width $W(\phi)$ versus ka at two different scattering angles with $\phi_0 = 90°$, and $r_0/\lambda = 10$, $(a_0\lambda)^2 = 0.053$, and $(b_0\lambda)^2 = 0.236$ for the Gaussian beam. (a) TM case. (b) TE case.

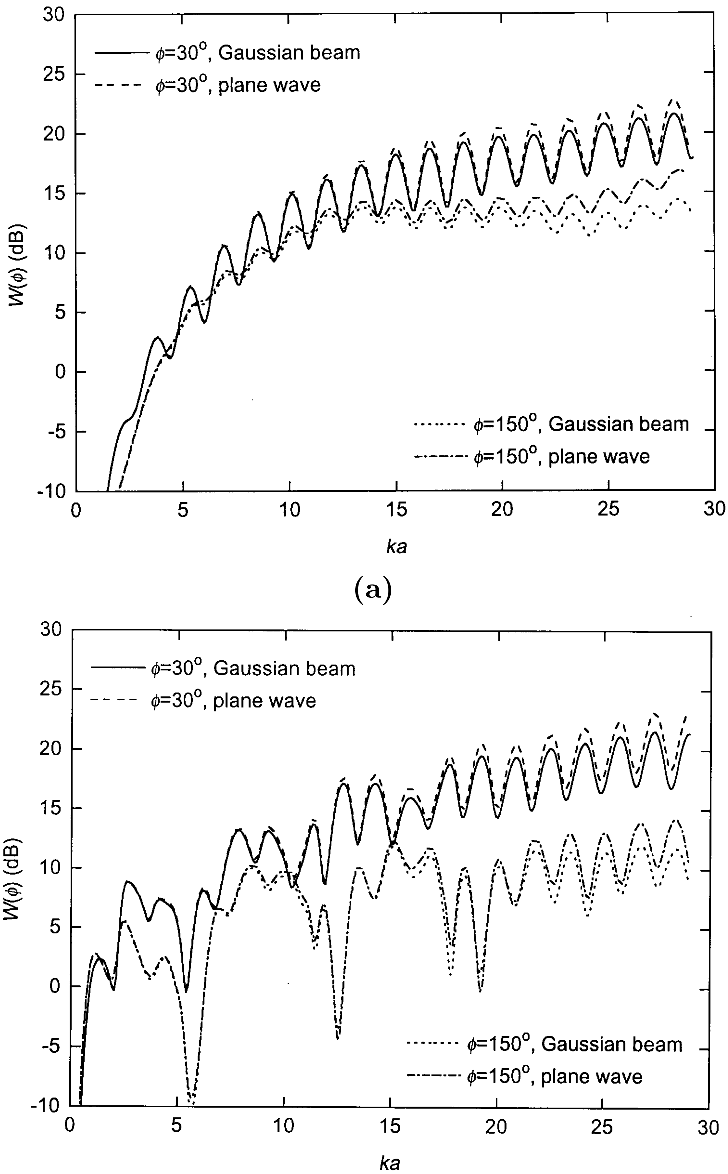

(a)

(b)

Figure 9. Scattering width $W(\phi)$ versus ka at two different scattering angles with $\phi_0 = 30°$, and $r_0/\lambda = 10$, $(a_0\lambda)^2 = 0.053$, and $(b_0\lambda)^2 = 0.236$ for the Gaussian beam. (a) TM case. (b) TE case.

REFERENCES

1. Sachdeva, B. K., and R. A. Hurd, "Scattering by a dielectric-loaded trough in a conducting plane," *J. Appl. Phys.*, Vol. 48, No. 4, 1473–1476, April 1977.
2. Hinders, M. K., and A. D. Yaghjian, "Dual-series solution to scattering from a semicircular channel in a ground plane," *IEEE Microwave Guided Wave Lett.*, Vol. 1, No. 9, 239–242, September 1991.
3. Park, T. J., H. J. Eom , W.-M. Boerner, and Y. Yamaguchi, "TM scattering from a dielectric-loaded semi-circular trough in a conducting-plane," *IEICE Trans. Commun.*, Vol. E75-B, No. 2, 87–91, February 1992.
4. Park, T. J., H. J. Eom, Y. Yamaguchi, W.-M. Boerner, and S. Kozaki, "TE-plane wave scattering from a dielectric-loaded semi-circular trough in a conducting plane," *J. Electromagn. Waves Applicat.*, Vol. 7, No. 2, 235–245, 1993.
5. Ragheb, H. A., "Electromagnetic scattering from a coaxial dielectric circular cylinder loading a semicircular gap in a ground plane," *IEEE Trans. Microwave Theory Tech.*, Vol. 43, No. 6, 1303–1309, June 1995.
6. Kozaki, S., "A new expression for the scattering of a Gaussian beam by a conducting cylinder," *IEEE Trans. Antennas Propagat.*, Vol. AP-30, No. 5, 881–887, September 1982.
7. Eom, H. J., G. Y. Hur, T. J. Park, and S. Kozaki, "Gaussian beam scattering from a semicircular boss above a conducting plane," *IEEE Trans. Antennas Propagat.*, Vol. 41, No. 1, 106–108, January 1993.